

# Experimental and Numerical Investigation of 3D Acoustic Receptivity due to Localized Wall Roughness

by W. Würz<sup>1</sup>, S. Herr<sup>1</sup>, A. Wörner<sup>1</sup>, U. Rist<sup>1</sup>, S. Wagner<sup>1</sup> and Y.S. Kachanov<sup>2</sup>

<sup>1</sup> Institut für Aerodynamik und Gasdynamik Universität Stuttgart, Pfaffenwaldring 21,  
70550 Stuttgart, Germany

<sup>2</sup> Institute of Theoretical and Applied Mechanics, Russian Academy of Science,  
630090 Novosibirsk, Russia

**Abstract.** Hot-wire measurements are performed on linear 3D acoustic receptivity in a two-dimensional laminar boundary layer. A localized quasi steady surface roughness serves as the receptivity element. A plane acoustic wave with frequency  $f_{ac}$  scatters at this vibrating source and the generated TS-wave train is measured downstream in spanwise cuts and at combination frequencies  $f_{1,2} = f_{ac} \pm f_v$ . After Fourier decomposition linear stability theory is used for upstream extrapolation to the initial amplitudes at the roughness element. The dispersion characteristic is determined and the complex receptivity function is calculated by normalization of the initial TS-spectra with the related amplitudes and phases of the surface vibrator and the acoustics. Three different acoustic frequencies were investigated and the results are compared with Direct Numerical Simulations based on a vorticity-velocity formulation of the complete Navier-Stokes equations and a new embedded wall model. Good quantitative agreement is achieved for the amplitude part of the receptivity function as well as for the phase part. The frequency dependence and the increase of the receptivity coefficients with spanwise wavenumber is found to be similar to results for vibrational receptivity.

## Introduction

The problem of boundary layer transition from laminar to turbulent flow still attracts much attention because of its fundamental and practical importance. It has three main aspects. First, there is the laminar flow receptivity to external perturbations. The second aspect is the linear development of boundary layer instabilities according to linear stability theory and finally there is the nonlinear flow breakdown to turbulence. This paper is devoted to experimental and numerical investigations of the linear 3D acoustic receptivity of a two-dimensional laminar boundary layer in the presence of a localized (3D) quasi steady surface non-uniformity.

This problem is poorly studied, so far. Most of the previous experiments in this field were devoted to two-dimensional receptivity problems (see e.g. [1], [2]). The quantitative receptivity characteristics of the 2D (Blasius) boundary layer to 3D surface vibrations were studied experimentally in [3]. The only available experimental investigation of the 3D vibrational acoustic receptivity was carried out in a swept-wing boundary layer and was devoted to the generation of cross-flow instability modes [4]. Recently, the acoustic receptivity due to stationary, localized 3D roughness was studied qualitatively in [5]. The

first quantitative evaluation of the complex 3D acoustic receptivity function was performed in [6] for quasi stationary 3D roughness and a single acoustic frequency.

In general, the amplitude part of the acoustic receptivity coefficient is defined by the ratio of the initial (i.e. at the surface non-uniformity) instability wave amplitude, generated in the boundary layer, to the amplitude of the external acoustic perturbation and the amplitude of the involved surface non-uniformity (see e.g. [7], [8], [4]). More exactly, all these amplitudes must be determined for every single (normal) mode of the corresponding frequency-wavenumber spectra, i.e. the spectra of the instability waves, surface non-uniformities and acoustic perturbations.

## Experimental Investigation

The experiments were carried out in the Laminar Wind Tunnel (LWT) of the IAG. The LWT is an open return tunnel with a turbulence level less than  $Tu = 2 \cdot 10^{-4}$ . The boundary layer measurements were performed on a symmetrical airfoil section at zero angle of attack and at a Reynolds number of  $1.2 \cdot 10^6$  based on the arclength  $s_{max} = 0.615 m$  measured from the leading edge (Fig. 1). A plane acoustic wave with fixed frequency was chosen as the external perturbation. In extension to [6], three different acoustic frequencies ( $f_{ac} = 720 / 1088 / 1562 Hz$ ) were used to cover a significant part of the unstable TS-frequency range for the selected boundary layer properties. The center frequency  $f_{ac} = 1088 Hz$  is close to the most unstable TS-frequency (with respect to the amplitude at the last measurement station). The acoustic wave was generated by a loudspeaker at the centerline downstream of the test section. The position of the localized 3D roughness element was selected to lie on branch I for  $f_{ac} = 1088 Hz$  (Fig. 2).

When studying 3D roughness acoustic receptivity, the data analysis represents a very complicated problem because of difficulties to distinguish signals measured at the same (acoustic) frequency but having different physical nature. The signal consists of a mixture of: (i) the instability wave generated by the acoustics (that is relatively weak initially), (ii) vibrations of the hot-wire probe and the model surface, and (iii) the acoustic field itself including the Stokes layer in the near-wall region. These experimental problems have been solved in [4] by means of arranging an unsteady surface non-uniformity (vibrating source) oscillating with a very low frequency and providing a quasi-steady scattering of the acoustic wave. A similar method has been applied in the present investigation. The vibrating source is driven at the frequency  $f_v = 1/64 f_{ac}$  which leads to an amplitude modulation of the generated 3D TS-wave in time. This corresponds to distinct combination modes in the frequency spectrum of the hot-wire signal at frequencies  $f_{1,2} = f_{ac} \pm f_v$ . In contrast to the signal observed at the acoustic frequency, the combination harmonics correspond to the instability waves *only*. The spatial behavior of these combination modes has been studied in detail.

The 3D roughness element was modeled by the inflection of the membrane of a circular surface vibrator. The active diameter ( $d = 6 mm$ ) was chosen to be approximately one half of the TS-wavelength (at  $f_{ac} = 1088 Hz$ ). The body of the source was set up flush-mounted with the model surface. The vinyl membrane was driven by a loudspeaker and the shape of the inflection of the membrane was measured with a laser triangulation device.

An acoustic amplitude of  $100 dB$  was used together with a vibrational amplitude of  $29.7 \mu m_{RMS}$  in order to be in the linear regime of receptivity and linear development of boundary layer instabilities.

The acoustic frequency as well as the vibrational frequency and the sampling trigger were generated strictly phase locked by a single time source. The ratios between the frequencies were chosen as integer powers of two ( $f_v : f_{ac} : f_{sample} = 1:64:8$ ) which gave the possibility to represent each of them with single Fourier coefficients after a FFT.

The initial amplitudes (which are necessary for determining the receptivity coefficients) of the most unstable TS-waves can not be measured directly in the flow because in the near-field of the source a mixture of different other perturbations such as continuous-spectrum instability modes and forced (bounded) fluctuations is present. Therefore, similar to some previous receptivity experiments (see e.g. [3]), we used the boundary layer as a selective amplifier of the most unstable (discrete-spectrum) modes and, simultaneously, an attenuator of the continuous-spectrum modes and the forced oscillations. The distributions of the TS amplitudes and phases were measured downstream of the surface non-uniformity. In contrast to [3] the linear stability theory was then used for extrapolation of the data to the position of the surface non-uniformity.

The hot-wire measurements were performed in 8 to 9 spanwise scans covering the whole width of the wave train. A constant, nondimensional wall distance of  $y/\delta_2 = 2.2$  was used in order to be close to the maximum of the TS-eigenfunction for different propagation angles. This procedure yields a good compromise for  $f_{ac} = 720 \text{ Hz}$  and  $f_{ac} = 1088 \text{ Hz}$  but obviously underpredicts (by up to 10%) the receptivity for  $f_{ac} = 1562 \text{ Hz}$  at propagation angles close to zero. A possible correction based on linear stability theory was not performed.

The time signals at every measurement point were analyzed with an FFT and the amplitude and phase of the perturbations obtained at the combination frequencies  $f_{1,2}$  were used for further data processing. The amplitudes were normalized by the local free-stream velocity  $U_\delta = 36 \text{ m/s}$  and the length with the displacement thickness  $\delta_{1ref} = 0.356 \text{ mm}$  ( $H_{12} = 2.57$ ) at the position of the source. The resulting spatial field of the disturbance amplitude for the "left" combination mode  $f_1 = f_{ac} - f_v$  is shown in Fig. 3.

## Experimental Results

The complex values of the wave train in physical space were mapped for each spanwise cut to spanwise wavenumber spectra. After this the downstream development of waves with different spanwise wavenumbers were investigated separately. The measured amplitudes (Fig. 4, symbols) for the combination modes are found to be consistent with the linear stability theory (Fig. 4, lines). This allows an upstream extrapolation to the position of the receptivity element. The associated phases could easily be fit by a straight line. The gradient of this line is the streamwise wavenumber  $\alpha_r$ . By this procedure the dispersion characteristic  $\alpha_r = \alpha_r(\beta)$  is determined that gives a dispersion relationship between the streamwise and spanwise wavenumbers (Fig. 5). From the double Fourier decomposition of the shape of the membrane oscillation the complex wavenumber spectrum of the surface vibration is obtained. From this spectrum the amplitudes of the "resonant" vibrational modes, that have the same wavenumbers as the TS-waves generated by them, can be found with the help of the dispersion function. Thus, the complex receptivity function  $\tilde{G}_{av,12}(\alpha_r, \beta)$  can be evaluated by calculating its amplitude part and its phase part separately according to the following definition:

$$\tilde{G}_{av1,2}(\alpha_r, \beta) = G_{av1,2}(\alpha_r, \beta) \cdot e^{i\phi_{av1,2}(\alpha_r, \beta)} = \frac{\tilde{B}_{inTS1,2}(\alpha_r, \beta)}{\tilde{A}_{ac} \cdot \tilde{A}_v(\alpha_r, \beta)}$$

where  $\tilde{B}_{inTS}$  is the complex initial spectrum of TS-waves excited by the acoustics on the vibrator,  $\tilde{A}_{ac}$  is the complex acoustic amplitude, and  $\tilde{A}_v(\alpha_r, \beta)$  is the complex spectrum of the resonant vibrational modes. Figure 6 to 8 show the amplitude and phase parts of the complex receptivity function, for the three investigated frequencies, in dependence of the propagation angle  $\theta(\beta) = \arctan(\beta/\alpha_r)$  of the generated TS-wave. The results for both combination frequencies are plotted.

## Comparison with Direct Numerical Simulations

The DNS are based on the vorticity-velocity formulation of the complete Navier-Stokes equations using a uniformly spaced grid in streamwise and wall-normal direction and a spectral representation in spanwise direction, c.f. [9]]. The sound wave in the free stream is prescribed as a solution of the second Stokes' problem at inflow, and a *novel wall model* has been implemented and compared with standard first-order formulations that consider only a no-slip condition in wall-parallel directions. The use of a body-fitted coordinate system is avoided and the typically small surface roughness is simulated by non-zero velocity at the lowest row of grid points which are extrapolated from the field in such a way as to fulfill the no-slip condition on the surface of the roughness. Here, this is done using high-order polynomials which are consistent to the finite-difference representation of the flow field. However, the main difference between the new model and models found in literature is that it takes into account the no-slip condition for the wall-normal velocity on the roughness, as well. Thus, at least for higher surface roughness, this novel formulation should lead to more accurate results.

A Blasius boundary layer is assumed at the position of the roughness element and the receptivity coefficients are evaluated for the same nondimensional wall distance as in the experiment. The DNS were performed for steady roughness, three acoustic frequencies and three discrete spanwise wavenumbers which correspond to propagation angles of  $0^\circ$ ,  $25^\circ$  and  $45^\circ$ , respectively. All modes show good quantitative agreement with the experimental receptivity functions (c.f. Fig. 6-8)

## Conclusions

The linear 3D acoustic receptivity due to a localized quasi stationary roughness element was studied experimentally and theoretically for three different acoustic frequencies in the range of the most unstable TS-frequencies. The obtained results demonstrate that the scattering of the acoustic wave is significantly more effective for 3D surface non-uniformities rather than for 2D ones. Similar to the vibrational receptivity [3] the acoustic receptivity coefficients for all propagation angles increase with the acoustic wave frequency. The most significant frequency dependence is observed for strongly 3D modes. The phase delays of the generated TS-waves depend only weakly on the spanwise wavenumber and the frequency.

## Acknowledgment

This work was performed under grant of the German Research Council (DFG) and is a part of the research program 'Transition'. The contribution of Y. S. Kachanov was supported by SEW-Eurodrive and Volkswagen Stiftung.

## References

- [1] Kosorygin V.S., Levchenko V.Y., Polyakov N.F.: *On generation and evolution of waves in laminar boundary layer*; In: Laminar-Turbulent Transition (Ed. V.V. Kozlov), pp. 233-242, Berlin: Springer, 1985
- [2] Saric W.S., Hoos J.A., Kohama Y.: *Boundary-layer receptivity: Part I: Freestream sound and 2D roughness strips*; Arizona State University, College of Engineering and Applied Sciences. Report CEAS-CR-R-90191, 1990
- [3] Ivanov A.V., Kachanov Y.S., Obolentseva T.G., Michalke A.: *Receptivity of the Blasius boundary layer to surface vibrations. Comparison of theory and experiment*; International Conference on Methods of Aerophysical Research, Proceedings Part I. - Novosibirsk: ITAM, pp.93-98, 1998
- [4] Ivanov A.V., Kachanov Y.S., Koptsev D.: *An experimental investigation of instability wave excitation in 3D boundary layer at acoustic scattering on a vibrator*; Thermophysics & Aeromechanics Vol. 4, No. 4, 1997
- [5] Cullen L.M., Horton H.P.: *Acoustic receptivity in boundary layers with surface roughness*, In: Laminar-Turbulent Transition (Eds.: Fasel H., Saric W.), IUTAM Symposium Sedona, Az./USA, Springer-Verlag Berlin, 1999
- [6] Würz W., Herr S., Wörner A., Rist U., Wagner S., Kachanov Y.S.: *Study of 3D Wall Roughness Acoustic Receptivity on an Airfoil*, In: Laminar-Turbulent Transition (Eds.: Fasel H., Saric W.), IUTAM Symposium Sedona, Az./USA, Springer-Verlag Berlin, 1999
- [7] Choudhari M., Streett C.L.: *A finite Reynolds-number approach for the prediction of boundary-layer receptivity in localized regions*; Physics in Fluids Vol. 11, pp. 2495-2514, 1992
- [8] Crouch J.D.: *Receptivity of three dimensional boundary layers*; AIAA Paper 93-0074, 1993
- [9] Rist U., Fasel H.: *Direct numerical simulation of controlled transition in a flat-plate boundary layer*; J. Fluid Mech. Vol. 298, pp. 211-248, 1995

## Figures

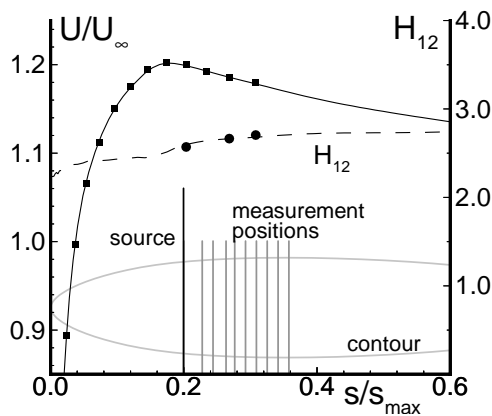


**Fig.1:** Pressure Distribution and airfoil contour

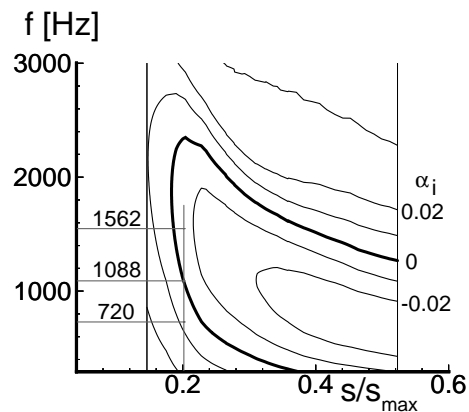


**Fig.2:** Stability diagram, roughness element at  $0.2 s/s_{max}$

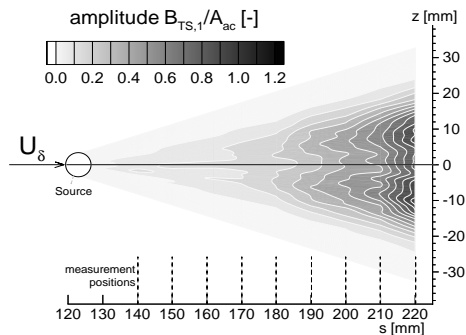


**Fig.3:** Amplitude part of the wave train (left combination mode, 1088 Hz)

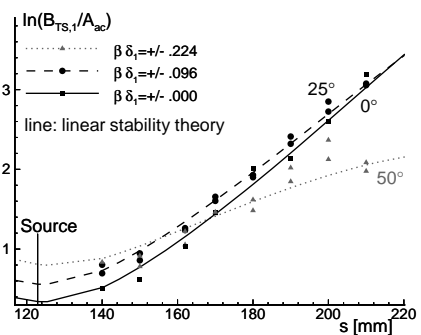


**Fig.4:** Comparison of amplitude development  $f_{ac}=1088 Hz$

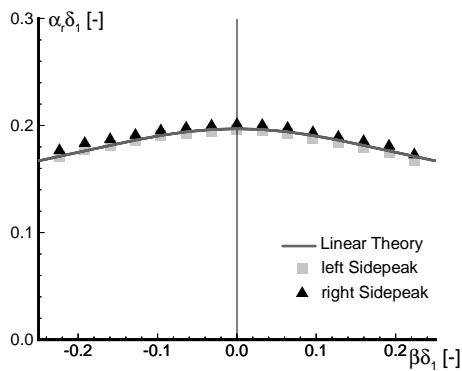


**Fig.5:** Dispersion characteristic at the position of the source (1088 Hz)

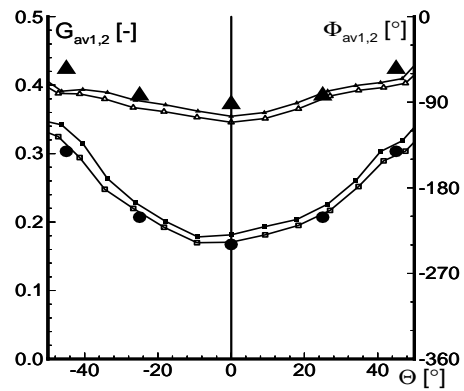


**Fig.6:** Amplitude and phase part of the receptivity function ( $f_{ac}=1088 Hz$ , Symbols: DNS)

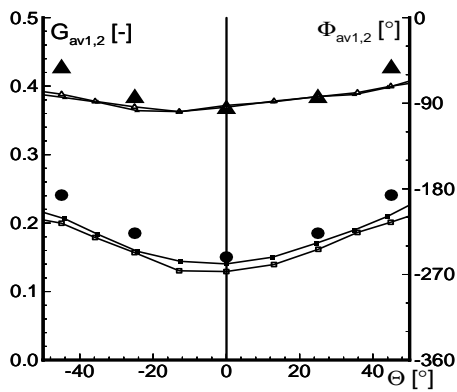


**Fig.7:** Amplitude and phase part of the receptivity function ( $f_{ac}=720 Hz$ , Symbols: DNS)

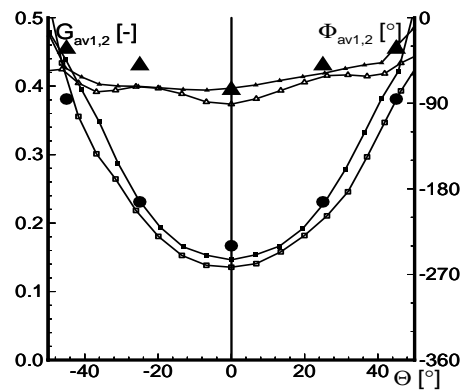


**Fig.8:** Amplitude and phase part of the receptivity function ( $f_{ac}=1562 Hz$ , Symbols: DNS)